J. Fluid Mech. (1967), *vol.* 30, *part* 3, *pp.* 513–531
Printed in Great Britain

The pipeline flow of capsules. Part 9†

By JAN KRUYER, P. J. REDBERGER AND H. S. ELLIS
Research Council of Alberta, Edmonton, Canada

(Received 20 February 1967)

The velocities and the associated pressure gradients of infinitely long liquid-borne cylinders flowing freely in pipes are related analytically to their radial positions. These velocities and pressure gradients are compared with those of liquids in cylinder-free pipes and expressed as ratios. A digital computer was used to evaluate the resultant equations for values of the cylinder/pipe diameter ratio between 0·25 and 0·97, with radial positions varying from the fully eccentric to the fully concentric position. As the clearance between the pipe and the bottom of the cylinder increases, the pressure ratio (R_P) decreases and the velocity ratio (R_V) increases. The relationship between R_P and R_V is independent of liquid viscosity and density, capsule density and pipe diameter, and is shown to be nearly linear for the larger diameter ratios. The R, R relationships are compared with data from three experimental capsule pipelines with pipe diameters from $\frac{1}{2}$ to 4 in., involving a variety of diameter ratios, cylinder lengths and densities, and oil viscosities. The experimental results for single capsules of finite length are shown to be in close agreement with the predictions for infinitely long cylinders.

The relevance of the analysis to capsule pipelining is indicated by relating experimental values of capsule velocity over a wide range of densities to the theoretical clearance of the capsules. A general relationship of this type would permit the optimization of the power requirements of any particular throughput of a given commodity.

1. Introduction

Capsule pipelining is a concept of economical long distance solids transport whereby the solids are introduced into the pipeline in the form of a long train of cylinders or spheres with diameters approaching that of the pipe. The capsules, which may be rigid slugs, flexible bodies of coherent paste, or packaged commodities, are carried along by the flowing liquid.

The concept of capsule pipelining was discussed in detail by Hodgson & Charles (1963). This was followed by a theoretical analysis by Charles (1963) of the concentric flow of long cylinders in pipes. The velocities of cylindrical and spherical capsules with the same density as the water carrier and also with densities greater than the water carrier, were measured in a $1\frac{1}{4}$ in. laboratory pipeline and reported by Ellis (1964*a–c*) as capsule/liquid velocity ratios.

† Parts 1 to 8 of this series have appeared in *The Canadian Journal of Chemical Engineering* under the title 'The pipeline flow of capsules'.

Similar experiments were made using an oil carrier to investigate effects of viscosity (Ellis & Bolt 1964; Round & Bolt 1965). A numerical analysis of some variables determining free flow of cylinders in laminar flow was presented by Newton, Redberger & Round (1964).

The design of commercial capsule pipelines requires a knowledge of liquid and capsule velocities and pressure gradients, and the present paper presents a means whereby these may be correlated. The first part of the paper consists of an analytical analysis of the movement of infinitely long cylinders in laminar flow in pipes and extends the analysis by Newton *et al.* The present analysis has been tested against a great variety of experimental data derived from three pipelines of diameters from $\frac{1}{2}$ to 4 in., and with cylindrical capsules of lengths from 3 in. to 4 ft. These supporting data are found in the second part of the paper. The clearance between the bottom of the cylinder and the pipe wall, rather than eccentricity, is adopted as the basic parameter throughout the paper since it is felt that this facilitates the application of lubrication theory to capsule flow and allows simpler comparisons between the theory and experimental measurements. Such practical matters as the effect of capsule density and surface roughness are also considered.

2. Analysis of the flow of infinitely long cylinders in laminar flow

The free flow of a cylinder in a pipe may be regarded as embracing a spectrum of positions of the cylinder bounded at the one limit by the concentric position and at the other by the fully eccentric position. The flow may be divided into two parts, the movement of the cylinder, expressed as a volumetric flow rate Q_c and the flow of the liquid in the annulus Q_A. In all cases for the movement of an infinitely long cylinder we have:

$$Q_c = \tfrac{1}{4}\pi d^2 V_c,$$

where d = cylinder diameter and V_c = cylinder velocity.

Laminar flow in the annulus of a free-flowing concentric cylinder was treated analytically by Charles (1963) and is given by

$$Q_A = B\left(\frac{dP}{dz}\right)_c (1-k^2)^2, \tag{1}$$

where $$B = -\frac{\pi g D^4}{108\mu},$$

$(dP/dz)_c$ = pressure gradient per unit length of annulus,

D = internal diameter of the pipe,

μ = absolute fluid viscosity,

$k = d/D$.

It may be shown that the concentric movement of the cylinder is given by

$$Q_c = B\left(\frac{dP}{dz}\right)_c (1-k^2)\,2k^2. \tag{2}$$

Bentwich, Kelly & Epstein (1966) derived an analytical expression describing the laminar flow conditions in the annulus of a pipe with an infinitely long free-flowing cylinder:

$$Q_A = B\left(\frac{dP}{dz}\right)_c \left[(1-k^2)^2 + 2k^2\epsilon^2 - \{8k\sinh(\alpha+\beta)\} \times \left\{\sum_{n=1}^{\infty}[\coth n(\alpha-\beta)]\left[\frac{2(n\epsilon\sinh\beta - k^2}{e^{2n\beta}+e^{2n\alpha}} + \frac{k^2}{e^{2n\alpha}}\right]\right\}\right], \tag{3}$$

where $\alpha = \cosh^{-1}\left\{\frac{1-k^2-\epsilon^2}{2k\epsilon}\right\}$ and $\beta = \cosh^{-1}\left\{\frac{1-k^2+\epsilon^2}{2\epsilon}\right\}$,

ϵ = distance between the axes of the pipe and the cylinder expressed as a fraction of the pipe radius,

n = integer.

For the movement of the cylinder Bentwich *et al.* obtained:

$$Q_c = B\left(\frac{dP}{dz}\right)_c \{4k^3\sinh(\alpha-\beta)\}. \tag{4}$$

Equations (3) and (4) simplify to (1) and (2) respectively for concentric cylinder flow but become indeterminate for fully eccentric cylinders. The case of a fully eccentric fixed cylinder was studied analytically by Caldwell (1930), and the flow rate is given by

$$Q_A = B\left(\frac{dP}{dz}\right)_c \left\{1-k^4-4k^2(1-k)^2\sum_{n=0}^{\infty}\frac{1}{(1+n-nk)^2}\right\}. \tag{5}$$

For a cylinder parallel to the pipe, the displacement, or eccentricity, ϵ, implicit in (3) and (4), is the distance between the axes of the cylinder and the pipe expressed as a fraction of the pipe radius. This may be related to C, the minimum clearance between the pipe and cylinder walls, expressed as a fraction of the pipe diameter:

$$\epsilon = 1-k-2C.$$

It has been found convenient to relate the velocity of the liquid-borne cylinder to the bulk velocity of the liquid flowing in the cylinder-free pipe, the volumetric flow rates in the two systems being equal. Equality of volumetric flow rate means that the combined flow rate of the cylinder and the annular liquid is equal to the flow rate in the cylinder-free pipe. The velocity ratio may therefore be expressed as

$$R_V = \frac{4Q_c/\pi d^2}{4(Q_c+Q_A)/\pi D^2} = \frac{Q_c}{k^2(Q_c+Q_A)}. \tag{6}$$

Similarly, the pressure ratio is defined as the pressure gradient in a pipe containing a cylinder, divided by the pressure gradient in a pipe without a cylinder for the same total volumetric flow rate. From (3) and (4) the flow rate of a cylinder plus the liquid in the annulus is

$$Q_c+Q_A = B\left(\frac{dP}{dz}\right)_c f(k,\epsilon). \tag{7}$$

In a cylinder-free pipe the flow rate is

$$Q_P = B\left(\frac{dP}{dz}\right)_P, \tag{8}$$

where $(dP/dz)_P$ = pressure gradient per unit length of pipe. Equating the flow in the free pipe with the flow of the cylinder plus the flow in the annulus (equations (7) and (8)) gives the pressure ratio at constant throughput

$$R_P = \left[\frac{(dP/dz)_c}{(dP/dz)_P}\right]_{Q=\text{const.}} = \frac{1}{f(k,\epsilon)}. \tag{9}$$

On the other hand, equating the pressure gradients, instead of the flow rates, gives the flow ratio at constant pressure gradient

$$\left[\frac{Q_P}{Q_c+Q_A}\right]_{dp/dz=\text{const.}} = \frac{1}{f(k,\epsilon)}. \tag{10}$$

Comparison of (9) and (10) shows that for a given capsule–pipe diameter ratio and clearance, the pressure ratio at constant throughput is equal to the flow ratio at constant pressure gradient or

$$R_P = \left[\frac{Q_P}{Q_c+Q_A}\right]_{dp/dz=\text{const.}}. \tag{11}$$

The velocity ratio and the pressure ratio for a concentric, free-flowing cylinder were given by Charles (1963) and may also be obtained from (1), (2), (6), (8) and (11). These are

$$R_{V(\text{con})} = \frac{2}{1+k^2} \tag{12}$$

and

$$R_{P(\text{con})} = \frac{1}{1-k^4}. \tag{13}$$

At the other limit the cylinder is fully eccentric and stationary and therefore the velocity ratio is zero. The pressure ratio may then be obtained from (5), (8) and (11). The infinite series of (5) converges very slowly but may be conveniently evaluated by substituting specific values for k, i.e. $k = (m-1)/m$, where m is an integer. For these values the series may be simplified as follows:

$$\sum_{n=0}^{\infty} \frac{1}{(1+n-nk)^2} = \sum_{n=0}^{\infty} \frac{m^2}{(m+n)^2} = m^2\left[\sum_{1}^{\infty}\frac{1}{n^2} - \sum_{1}^{m-1}\frac{1}{n^2}\right]$$

$$= m^2\left[\frac{\pi^2}{6} - 1 - \frac{1}{2^2} - \frac{1}{3^2} - \cdots - \frac{1}{(m-1)^2}\right].$$

Table 1 shows a number of values of m, k and R_P for fully eccentric cylinders; the values of R_P for k equal to 0·100 and 0·300 have been evaluated by using the infinite series of (5). A curve fitted to these values (figure 5) yielded:

$$R_{P(\text{ecc})} = 0{\cdot}645 + \frac{0{\cdot}355}{(1-k)^{2{\cdot}95}}, \tag{14}$$

which agrees within 2 % or better with the analytical solution for values of k greater than 0·4. For smaller values of k the analytical solution needs to be evaluated.

The velocity ratio and pressure ratio between the two clearance extremes may be evaluated from (3), (4), (6) and (11). For the present study, values of velocity ratio and pressure ratio were obtained for diameter ratios varying from 0·25 to 0·97 for a number of cylinder clearances, C. Table 2 gives the values of the cylinder clearances for various values of a parameter N arbitrarily chosen for convenience of calculation.

m	k	R_P
1	0·000	1·00
	0·100	1·06
	0·300	1·58
2	0·500	3·42
3	0·667	9·96
4	0·750	22·2
5	0·800	42·0
10	0·900	316·0
20	0·950	2462·0

TABLE 1. Pressure ratios for fully eccentric cylinders evaluated from (5), (8) and (11)

N	$C = \frac{2^N}{1000}$ pipe diameters	N	$C = \frac{2^N}{1000}$ pipe diameters
−9	$1{\cdot}953 \times 10^{-6}$	0	$1{\cdot}000 \times 10^{-3}$
−8	$3{\cdot}907 \times 10^{-6}$	1	$2{\cdot}000 \times 10^{-3}$
−7	$7{\cdot}813 \times 10^{-6}$	2	$4{\cdot}000 \times 10^{-3}$
−6	$1{\cdot}563 \times 10^{-5}$	3	$8{\cdot}000 \times 10^{-3}$
−5	$3{\cdot}125 \times 10^{-5}$	4	$1{\cdot}600 \times 10^{-2}$
−4	$6{\cdot}250 \times 10^{-5}$	5	$3{\cdot}200 \times 10^{-2}$
−3	$1{\cdot}250 \times 10^{-4}$	6	$6{\cdot}400 \times 10^{-2}$
−2	$2{\cdot}500 \times 10^{-4}$	7	$1{\cdot}280 \times 10^{-1}$
−1	$5{\cdot}000 \times 10^{-4}$	8	$2{\cdot}560 \times 10^{-1}$

TABLE 2. Values of the clearances between cylinder and pipe wall used in the calculations and in figures 4–7

The infinite series was summed (IBM 1620 computer) to obtain the velocity ratios and pressure ratios. At large clearances the series converged rapidly and for values of N greater than -3, eight-digit accuracy was used in the calculation, the series being terminated when the last term became smaller than 10^{-6}. At smaller clearances convergence was very slow; in some cases more than 1000 terms were required to reach the new termination point of 10^{-10}. An accuracy of 12 digits was used for the latter calculations.†

The effect of clearance on the velocity ratio

Figure 1 shows, for a number of diameter ratios, the relation between clearance and velocity ratio. In the one extreme, not shown in figure 1, all curves go to zero as C goes to zero and the cylinders are resting on the pipe wall. The other extreme represents concentric cylinders, i.e. maximum individual clearances. At

† A table of the calculated values may be obtained from the authors.

the maximum possible diameter ratio (1·0) the cylinder is a piston in the pipe and if it moves at all, the velocity ratio is 1·0. For any diameter ratio less than 1·0 the greater the clearance the greater the velocity ratio. This effect of clearance on the velocity ratio is more pronounced as the diameter ratio is decreased. This may be seen when comparing the curves for the 0·90 and 0·97 diameter

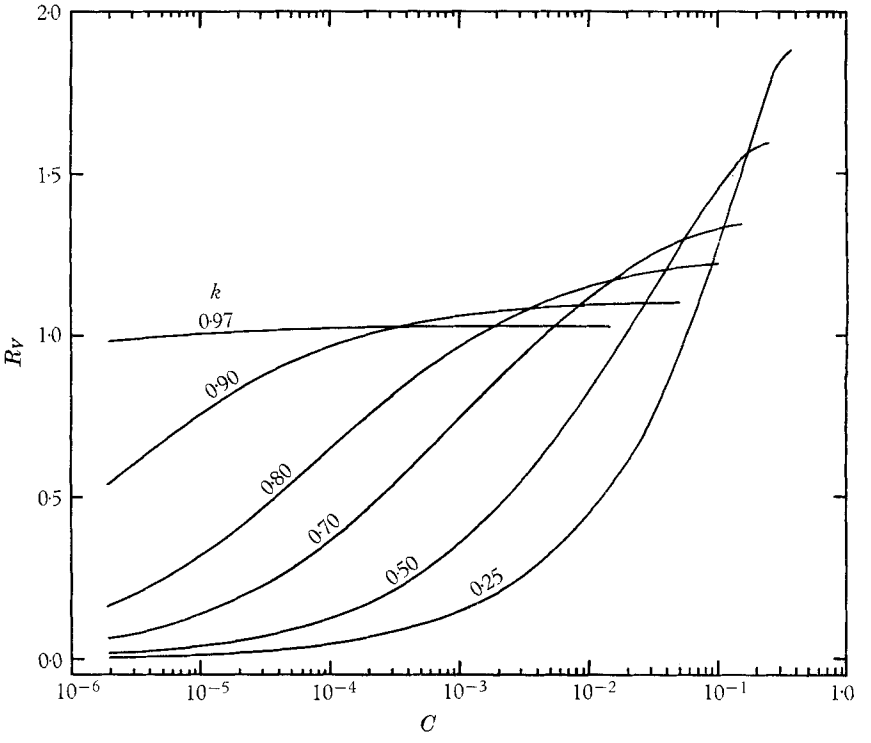

FIGURE 1. The predicted effect of clearance on the velocity ratio for diameter ratios from 0·25 to 0·97.

ratios. The velocity ratio for the smaller diameter ratio is 50 % of that for the larger one at the smallest clearance shown but rises more rapidly and surpasses it at a clearance of $3{\cdot}5 \times 10^{-4}$ pipe diameters. All the graphs in the figure show this overtaking in velocity ratio of larger diameter ratios by smaller diameter ratios as the clearance increases. Such an overtaking was observed experimentally by Ellis (1964*b*) for finite cylinders of different diameters as liquid velocities increased. In these experiments an increase of clearance was visible when the velocity ratio was increased.

Figure 2 shows the effect of clearance on the difference between the velocity ratio of a concentric cylinder and that of an eccentric cylinder of the same diameter ratio; both the ordinate and the abscissa are logarithmic scales. The new ordinate eliminates the intersecting curves of figure 1 and thereby simplifies estimating values of velocity ratio for intermediate diameter ratios. Velocity ratios for the commercially interesting larger diameter ratios may also be obtained more accurately by the use of figure 2.

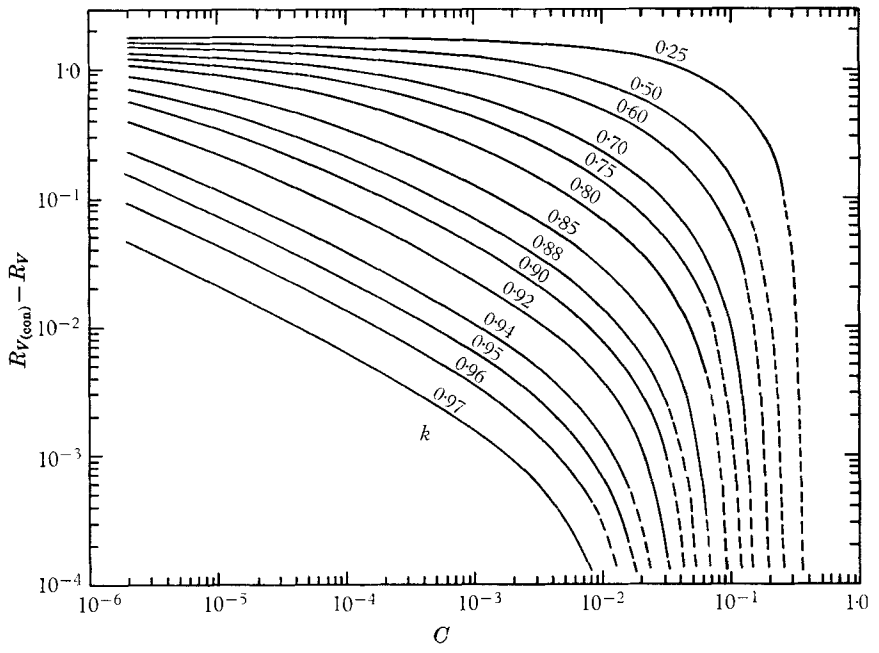

FIGURE 2. The predicted difference between the velocity ratios of a concentric cylinder and of an eccentric cylinder as a function of clearance for diameter ratios from 0·25 to 0·97.

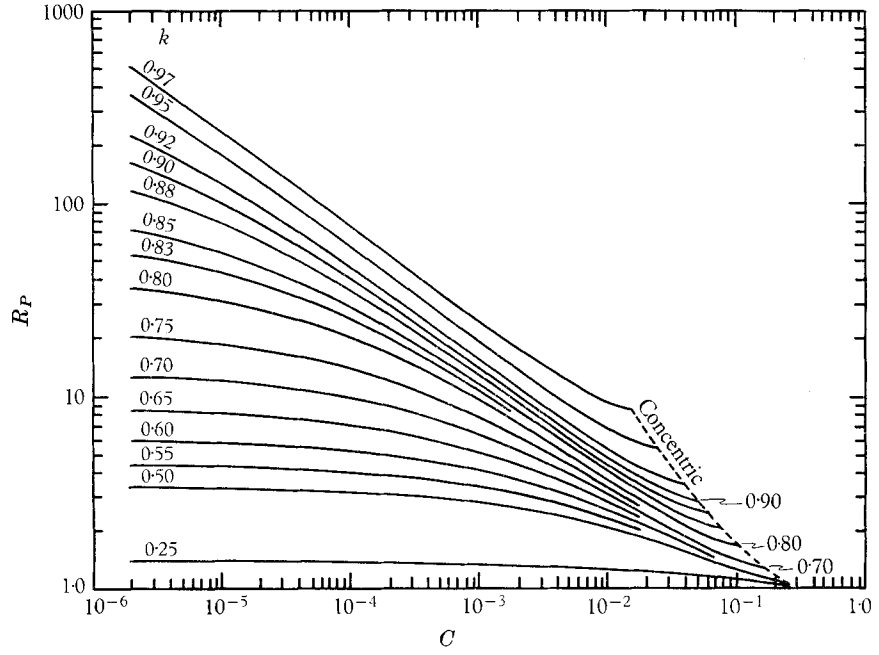

FIGURE 3. The predicted effect of clearance on the pressure ratio for diameter ratios from 0·25 to 0·97.

The effect of clearance on the pressure ratio

The relation between clearance and pressure ratio is shown by figure 3 for a number of diameter ratios. As may be seen when comparing the uppermost curves with the bottom curves, the pressure ratios for the large diameter ratios are much more dependent on clearance than are those for the small diameter ratios.

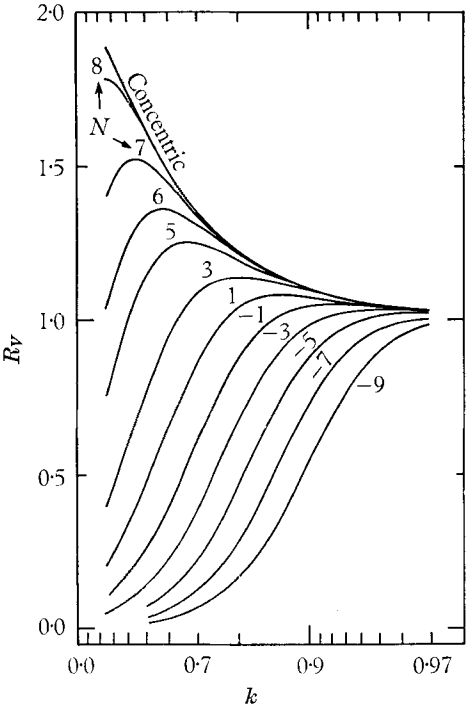

FIGURE 4

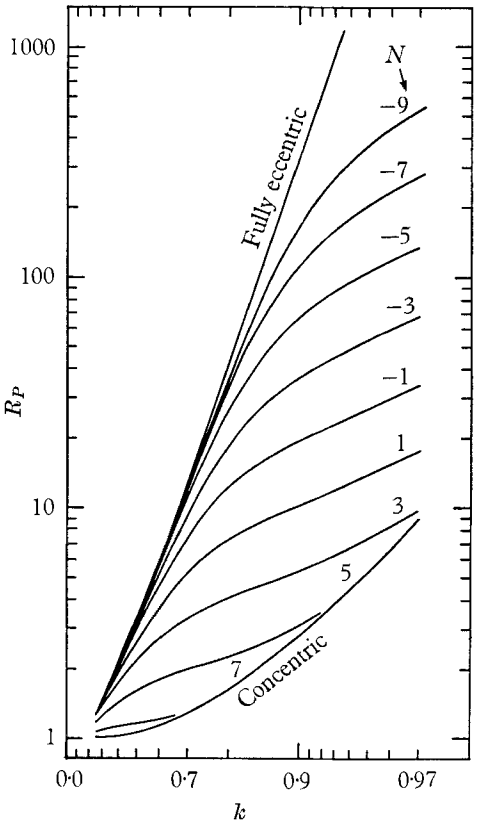

FIGURE 5

FIGURE 4. The predicted effect of diameter ratio on the velocity ratio for a number of cylinder positions corresponding to the values of N given in table 2.

FIGURE 5. The predicted effect of diameter ratio on the pressure ratio for a number of cylinder positions as given in table 2.

The curves in figures 1–3 terminate at a clearance of about 2×10^{-6} pipe diameters which is smaller than the relative roughness of drawn tubing. Undoubtedly in actual practice the pipe and cylinder roughnesses will affect the velocity ratios and pressure ratios at the smaller clearances.

The effect of diameter ratio on the velocity ratio

The effect of diameter ratio on the velocity ratio is shown in figure 4 for a number of cylinder clearances. The clearances are indicated by values of N as defined in table 2. The abscissa indicates values of k on a logarithmic scale of $1/(1-k)$.

The ends of the curves are not shown in figure 4. On the right-hand side they all meet at a velocity ratio of 1·0 for a diameter ratio of 1·0. On the left-hand side the diameter ratio goes to zero and the velocity ratio becomes the velocity of an individual stream line for ideal laminar flow divided by the average liquid velocity:

$$R_V = 8C(1-C).$$

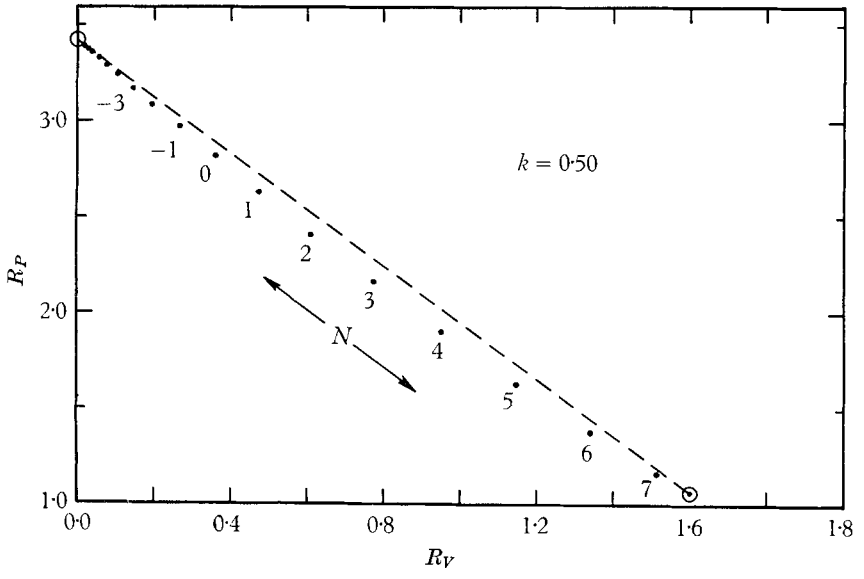

FIGURE 6. The predicted velocity ratios and pressure ratios for a 0·50 diameter ratio cylinder for positions corresponding to the values of N given in table 2. The fully eccentric and concentric positions are marked by circles and are joined by the dashed line.

The curves show that for a given clearance there is a diameter ratio that gives the maximum velocity ratio for that clearance. During experimental pipeline flow studies of deformable cylinders of finite lengths Berkowitz, Brown & Jensen (1965) observed a deformation of the cylinders toward a constant diameter ratio of 0·80. It may well be that a connexion exists between the experimentally observed diameter deformation and the optimum diameter ratios of figure 4.

The effect of diameter ratio on the pressure ratio

The relation between diameter ratio and pressure ratio is shown in figure 5 for a number of cylinder positions. The uppermost curve represents the pressure ratio for fully eccentric cylinders at rest. The pressure ratio for such cylinders of any diameter ratio may be obtained for design purposes from (14). The bottom curve shows the pressure ratios for concentric cylinders flowing freely in the pipe.

Relating the four variables

Figure 6 is a plot of the pressure ratio versus the velocity ratio for various cylinder positions for a diameter ratio of 0·5. The circle on the y-axis represents the pressure ratio for a fully eccentric cylinder and the circle to the right on the

bottom of the figure represents the pressure and velocity ratios for a concentric cylinder. A straight dashed line is shown connecting the two extremes. Similar figures may be drawn for other diameter ratios and they all show a maximum difference of about 8 % between the straight line and the points at about the same clearance ($N = 4$). For the large diameter ratios, which show high pressure ratios at the low clearances, the 8 % difference at small pressure ratios (at $N = 4$) is negligible when considering the over-all curve and then the R_P versus R_V curve may be approximated by the straight line.

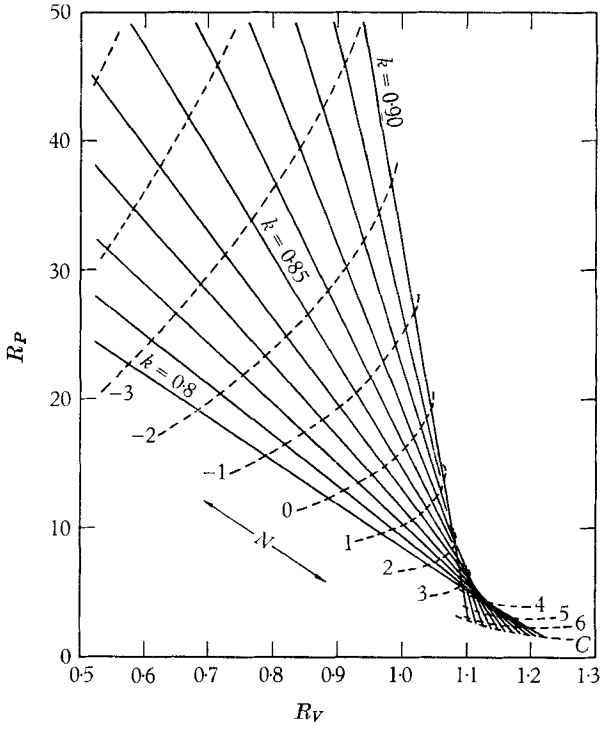

FIGURE 7. The predicted velocity ratios and pressure ratios for diameter ratios from 0·80 to 0·90 for cylinder positions corresponding to the values of N given in table 2.

Figure 7 is a composite velocity ratio, pressure ratio plot for a number of diameter ratios between 0·8 and 0·9. The curves intersect and the plot appears to be a projection of a three-dimensional surface. The third dimension is a function of clearance and diameter ratio. Figure 7 presents a useful basis for correlating experimental data since it is independent of liquid properties, capsule density and pipe diameter. It also incorporates in one figure four variables (R_P, R_V, k and C) involved in the free flow of cylinders in pipes. When two variables are known, the other two may be predicted from the curves. This is especially useful in experimental work since the very small clearances may be difficult to measure to great accuracy, while accurate pressure and velocity ratios may often be determined more conveniently. However, it must be remembered that the curves refer to infinite cylinders flowing parallel to the pipe wall. In practice, capsules are finite and have been observed by Ellis (1964*b*) to flow in a slightly nose-up attitude.

3. Extending the prediction to turbulent flow in the free pipe

The foregoing theoretical relationships have been developed on the basis of laminar flow in the capsule-pipe annulus and in the free pipe; it is now possible to extend the theory to include a long cylinder in a pipe in which the liquid is in turbulent flow, but with the turbulence suppressed to give laminar flow in the cylinder-pipe annulus.

If the cylinder is long enough that the pressure losses due to disturbances at the ends are negligible compared with the pressure drop along the cylinder, the pressure gradient and velocity of the cylinder will not be affected by the turbulence in the free pipe. Experimental data secured under these conditions may then be compared with the foregoing laminar theory provided that the liquid pressure gradient term (dP/dz) in R_P is calculated by the Hagen–Poiseuille equation, as if the liquid in the free pipe were in laminar flow at the existing liquid velocity. By this device the R_P, R_V curve shows no discontinuity as long as the flow in the annulus remains laminar, the pressure gradient being compared with that in a free laminar liquid stream as before. Since it has been found experimentally (Ellis 1964*a*) that capsules of large diameter ratio do suppress turbulence in the annulus to a marked degree, the range of usefulness of the theoretical predictions can be extended into the turbulent pipe-flow régime found in commercial pipelines.

4. Experimental data

Experimental data were obtained for cylindrical capsule flow in three pilot-scale pipelines (table 3) under a large variety of conditions of pipe size, diameter ratio, capsule length and density, and liquid viscosity. These data for finite cylinders were compared with the theoretical predictions for infinite cylinders.

Liquid velocities were determined from calibrated flow meters, and capsule velocities from the transit time between two photocells. Liquid pressure gradients were correlated by means of a Reynolds number, friction factor plot. Capsule pressure gradients were calculated by measuring the increase in pressure due to the presence of the capsule in the test section, expressing this as a gradient by dividing it by the capsule length and then adding to this the measured liquid pressure gradient over the test section at the same flow rate, i.e.

$$\left(\frac{dP}{dz}\right)_c = \frac{\Delta P_c}{L_c} + \left(\frac{dP}{dz}\right)_p, \tag{15}$$

where ΔP_c = the increase in pressure due to the capsule. L_c = capsule length.

Data from a $\frac{1}{2}$ in. pipeline

Figures 8 and 9 present experimental data for 24 and 3 in. long cylinders respectively, flowing in a viscous lubricating oil (μ = 36 cP., liquid S.G. (ρ) = 0·86) in a $\frac{1}{2}$ in. pipeline (table 3). Flow was laminar in the pipe for the complete range of liquid velocities used. Loaded hollow cylinders were used in the experiments to obtain data for the same cylinder surface at different cylinder specific gravities

(σ). Three axes are used in the figures to represent a number of variables simultaneously. Arrows on the curves refer to the axes used to represent the variables. The dependence of one variable on the other may be understood by following the

Average internal pipe diameter in the test section (in.)	0·532	1·254	4·03
Diameter tolerance (in.)	0·001	0·01	0·02†
Pipe material	Copper (reamered)	Acrylic plastic	Steel
Test section length (ft.)	8·00	10·00	20·00
Upstream calming section (ft.)	12	21	110
Downstream calming section (ft.)	3	3	60

† Estimated.

TABLE 3. Pertinent data on the experimental capsule pipelines

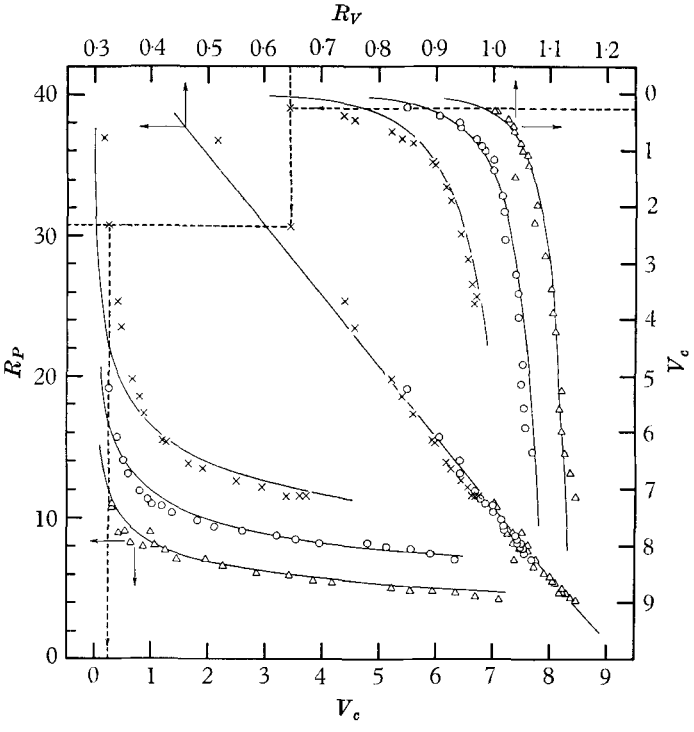

FIGURE 8. The experimentally measured velocity ratio, pressure ratio and capsule velocity of a 24·0 in. long 0·824 diameter ratio capsule flowing in lubricating oil (μ = 36 cP., ρ = 0·86) in a 0·532 in. diameter pipeline. The hollow cylindrical capsule was loaded to three specific gravities: △, 2·03; ○, 5·01; ×, 11·75. The straight line is the predicted R_P, R_V relationship for this diameter ratio and the curves are drawn by means of the correlation of figure 13.

dashed lines in figure 8. The nearly straight line in both figures which represents the theoretical prediction for the velocity ratio versus pressure ratio at a diameter ratio of 0·824 is very close to the experimental points for both the 24 in. (L_c/d = 55) and the 3 in. (L_c/d = 6·8) cylinders. Thus in this small diameter pipe

the effect of the cylinder ends, even on a cylinder as short as 3 in., does not cause much deviation from the theoretical R_P, R_V relationship for infinite cylinders.

The curved lines in figure 8 and 9 which are plots of pressure ratio and velocity ratio versus capsule velocity will be discussed further on.

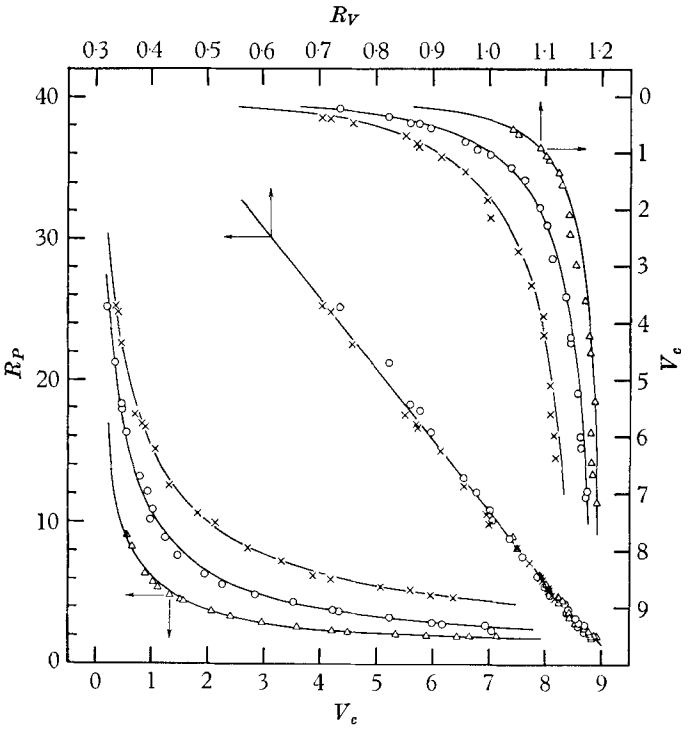

FIGURE 9. Experimental data as for figure 8 but with a 3·0 in. long cylinder of specific gravity: △, 2·67; ○, 5·32; ×, 10·0 respectively.

Data from a 1¼ in. pipeline

Figure 10 presents experimental data relating to 18 and 24 in. long hollow cylinders of three diameters, each cylinder being loaded to four specific gravities ranging from 1·92 to 7·84. The experiments were made in a 1¼ in. pipeline (table 3) using a viscous lubricating oil (μ = 28 cP., ρ = 0·855) with laminar flow in the free pipe at all liquid velocities. The lines show the analytical prediction for the three diameter ratios of 0·90, 0·70 and 0·50 respectively. The experimental points from this pipeline are further removed from the analytical prediction than those from the smaller diameter pipeline but there is still surprisingly close agreement between the theory for an infinitely long cylinder and experimental data from these finite capsules (L/d = 16 or 21), especially when the variation in the internal pipe diameter through the test section (table 3) is taken into consideration.

Four possible reasons may be cited for any discrepancies between data from cylindrical capsules and the theoretical predictions: (i) the experimental capsule is not infinite and may display end effects; (ii) the capsule axis is not parallel to

the pipe axis in most cases; (iii) when the capsule moves at very small clearances a friction force between the pipe wall and the capsule is introduced; and (iv) turbulence may be present in the annulus. Any one of these four conditions invalidates the analytical model of an infinitely long free-flowing cylinder in laminar flow. It is also possible that these four causes of deviation may at times compensate one another to give experimental data closer to the prediction than warranted.

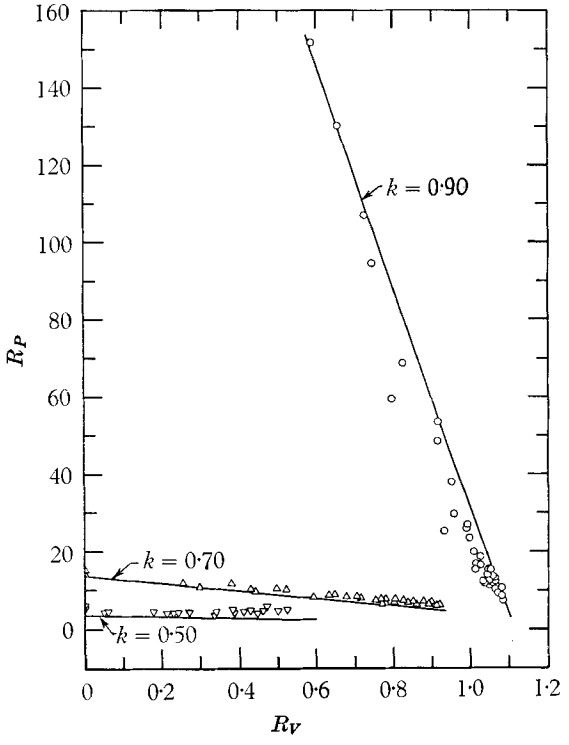

FIGURE 10. The experimentally measured velocity ratios and pressure ratios of capsules 18 in. long, 0·90 diameter ratio, 24 in. long, 0·70 diameter ratio and 24 in. long, 0·50 diameter ratio, flowing in lubricating oil (μ = 28 cP., ρ = 0·855) in a 1·25 in. diameter pipeline. The hollow cylindrical capsules were loaded to four specific gravities each, ranging from 1·92 to 7·84. ○, k = 0·90, L_c = 18 in.; △, k = 0·70, L_c = 24 in.; ▽, k = 0·50, L_c = 24 in.

Figure 11 shows experimental data from 18 in. solid steel, aluminium and acrylic plastic cylinders run in a light lubricating oil (μ = 5·7 cP., ρ = 0·828) in the $1\frac{1}{4}$ in. pipeline. The closed symbols represent the pressure ratios calculated as in figures 8–10 directly from the experimentally measured capsule and liquid pressure gradients. The oil velocities in the experiment (2·23–11·55 ft./sec) represented turbulent flow in the free pipe (Reynolds numbers varied from 3140 to 16,200), so that the analytical model of laminar flow both in the annulus and in the free pipe is no longer valid, and the experimental points are shown to deviate markedly from the line representing the analytical prediction. The open symbols in figure 11 ,which represent the pressure ratios calculated by means of the Hagen–Poiseuille equation, as explained previously, closely approach the

line showing the analytical prediction. However, when comparing these open symbols of figure 11 with the circles in figure 10, effects of some carry-over of turbulence from the free pipe into the annulus for the data involving the lighter oil are suggested by the higher pressure ratios over the whole range of velocity ratios.

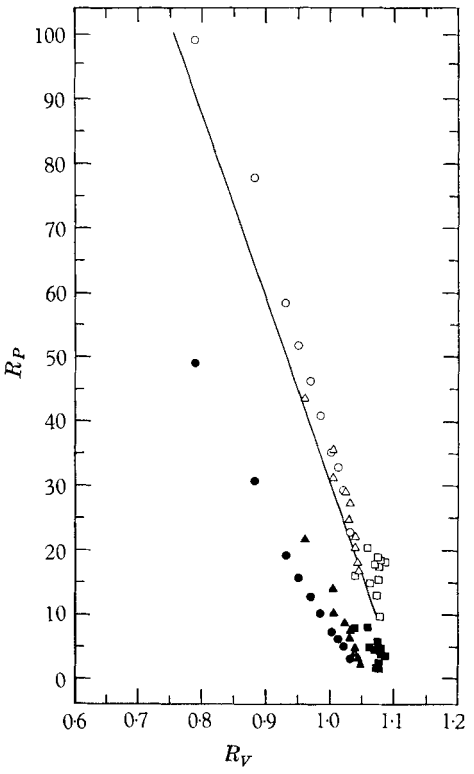

FIGURE 11. The experimentally measured velocity ratios and pressure ratios (shaded symbols) and the laminar–laminar pressure ratios calculated by means of the Hagen–Poiseuille equation (open symbols) of steel (circles), aluminium (triangles) and acrylic plastic (squares) 18 in. long, 0·90 diameter ratio capsules flowing in light lubricating oil (μ = 5·7 cP., ρ = 0·83) in a 1·25 in. diameter pipeline.

Data from a 4 in. pipeline

Figure 12 presents experimental data from a pipeline made of commercial 4 in. diameter steel pipe (table 3). The capsule was a 48 in. aluminium cylinder, diameter ratio 0·90 flowing in viscous transformer oil (μ = 16·7 cP., ρ = 0·853). Flow in the pipe was laminar at low liquid velocities but became turbulent at high velocities. Two symbols are used in the figure: crosses refer to the pressure ratios as calculated from the pressure gradients measured in the pipeline, and circles refer to the pressure ratios obtained when using laminar liquid pressure gradients to calculate the ratios as explained for the data of figure 11. Since the diameter ratio of the capsule in the test section depends on the variation of the inside diameter of the commercial pipe, which is not known exactly, the analytical predictions for diameter ratios of 0·91 and 0·89 are also given in the figure.

The theoretical clearances shown indicate that the thickness of the liquid layer under the capsule was very small. In fact, in all cases these clearances were less than the relative roughness usually ascribed to 4 in. commercial steel pipe ($4{\cdot}5 \times 10^{-4}$). While the pipe is probably worn and has a much lower relative roughness, the deviation on the figure between the circles and the prediction may be partly due to friction between the solid surfaces.

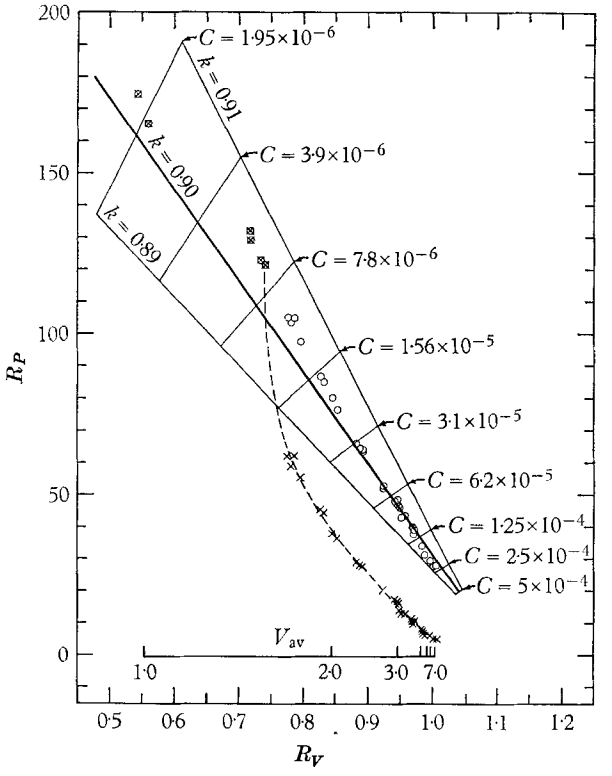

FIGURE 12. The experimentally measured velocity ratios and pressure ratios (crosses) and the laminar–laminar pressure ratios calculated by means of the Hagen–Poiseuille equation (circles) of a 48 in. long, 0·90 diameter ratio aluminium (σ = 2·71) cylindrical capsule flowing in transformer oil (μ = 16·7 cP., ρ = 0·853) in a 4·03 in. diameter pipeline.

It should be pointed out that theoretical clearances are used as the basis of the figures and that no attempt has been made as yet to measure clearances experimentally. The phenomenon of clearance between the cylinder and the pipe wall has been compared with that of the liquid wedge in a slipper bearing by Ellis (1964*b*). Undoubtedly the clearance between the moving cylinder and the pipe wall is not uniform over the capsule and in most cases is largest at the nose and smallest at the tail.

The scale, inserted at the bottom of figure 12, provides the relationship between the velocity ratio and pressure ratio of this particular capsule and the liquid velocity. For example, increasing the liquid velocity from 2·0 to

5·0 ft./sec results in a decrease in the measured pressure ratio from 39 to 7. The capsule velocity increases concurrently from 1·7 to 4·9 ft./sec, yielding nearly three times the throughput of aluminium.

5. Effect of the capsule specific gravity and velocity on clearance

Curves relating clearance to R_V and R_P have been presented in figures 1 and 3. If similar curves are drawn for the diameter ratio of figures 8 and 9, values of clearance can be read off corresponding to the measured values of R_P and R_V.

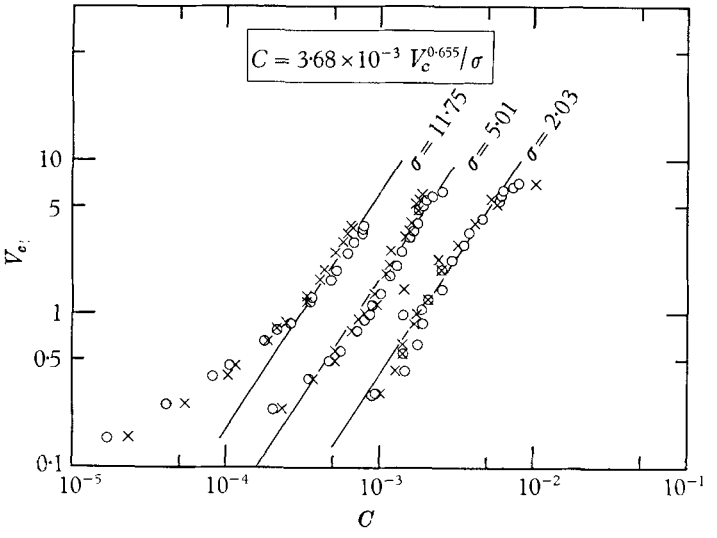

FIGURE 13. The experimentally measured capsule velocity as a function of the theoretical clearance of the 24·0 in. long, 0·824 diameter ratio capsule of figure 8. The theoretical clearances were obtained from a plot similar to figure 1 (circles) and also from a plot similar to figure 3 (crosses). $D = 0{\cdot}532$ in., $\rho = 0{\cdot}86$, $\mu = 36$ cP.

In figures 13 and 14 these clearances are plotted for the data from the $\frac{1}{2}$ in. pipeline against the corresponding capsule velocities. The circles in the figures refer to the clearance obtained from the R_V curve and the crosses refer to the clearance obtained from the R_P curve. It is evident that for any one capsule there is a close relationship between the capsule velocity and the theoretical clearance, whether the latter is obtained from the velocity ratio or the pressure ratio. Straight parallel lines drawn through the S-curves of figure 13 result in an empirical correlation for the clearance as a function of the cylinder velocity and specific gravity. Deviation from the straight line becomes very apparent for the most dense capsule at a clearance of about 2×10^{-4}, the dimension of the relative roughness of 'smooth' $\frac{1}{2}$ in. diameter pipes. It is probable that in the experimental runs roughnesses at the cylinder and pipe walls had an adverse effect on the capsule movement at these small clearances. In figure 14 where the fit is much more linear, the best straight line was drawn through the points for each specific gravity. When comparing figures 13 and 14 it may be interesting to note that a change in specific gravity generally tends to cause a parallel shift

of the straight lines while the effect of cylinder length is to change the slope of the lines.

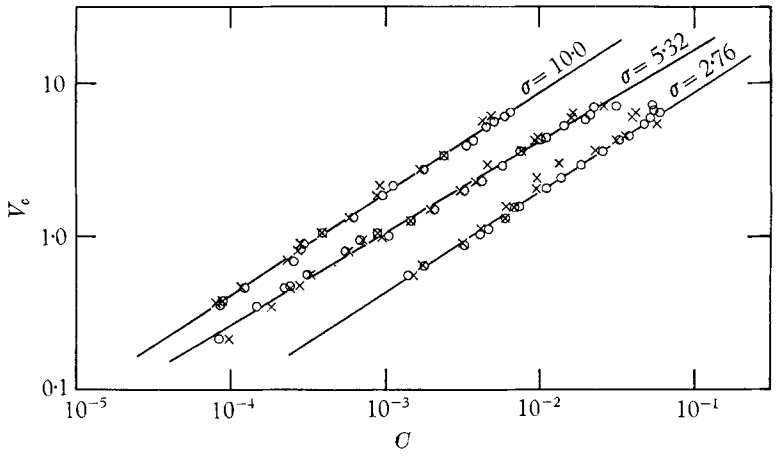

FIGURE 14. A plot similar to figure 13 but for the 3·0 in. capsule of figure 9. $D = 0{\cdot}532$ in., $k = 0{\cdot}824$, $L_c = 3{\cdot}0$ in., $\rho = 0{\cdot}86$, $\mu = 36$ cP.

6. Estimation of velocities and power requirements for capsule trains

Since for the long cylinders (figure 13) the straight lines give a simple relationship between clearance, cylinder velocity and specific gravity, such a relationship derived for a long capsule may be used to obtain a practical estimate of the pressures, velocities and power requirements for the movement of capsule trains assuming these will behave as if they were a single long capsule. Such a prediction would involve the following steps.

(i) The cylinder velocity is calculated from the desired solids throughput, the percentage of pipeline length occupied by capsules and trial capsule and pipe diameters.

(ii) A clearance is obtained from a correlation such as presented in figures 13 and 14.

(iii) The pressure ratio and the velocity ratio are obtained from theoretical plots such as presented in figures 1 and 3.

The curves in figures 8 and 9 were derived in this way for the cylinder specific gravities and lengths tested experimentally. The differences on the figures between the experimental points and the curves give some indication of the precision of such an estimate. Further steps required to obtain the capsule pressure gradient are the following.

(iv) The liquid bulk velocity is calculated from the velocity ratio and the capsule velocity; and the laminar liquid pressure gradient is calculated from the liquid velocity and viscosity and the pipe diameter by means of the Hagen–Poiseuille equations.

(v) The capsule pressure gradient is calculated from the pressure ratio and the liquid pressure gradient.

Finally, power requirements are calculated by the conventional means from

the total volumetric flow and the total pressure drop in the pipeline; the latter is obtained by summing the capsule pressure drops over each capsule and the liquid pressure drops over each space between capsules. Power per unit throughput can be optimized by selecting other diameter ratios or pipe diameters and recalculating the power requirements. If the capsule bulk specific gravity can be varied (e.g. by foaming) it may be used also as a means of optimizing power per mass throughput.

7. Conclusions

Although almost continuous trains of capsules would be employed in commercial capsule pipelines the performance of a single long cylinder provides a theoretical criterion against which the performance of a train of capsules can be judged. Experimental data from a large number of single capsules run in experimental capsule pipelines from $\frac{1}{2}$ in. to 4 in. in diameter show that good agreement exists between the analytical prediction and experimental data as long as liquid in the capsule–pipe annulus is in laminar flow and as long as clearances are large enough to maintain free-flow of the capsule.

An experimental relation between cylinder velocity and theoretical clearances suggests an approach whereby the many variables in capsule flow may be correlated. For when the capsule velocity and the theoretical clearance of a required capsule system are known, liquid velocity, pipeline pressure gradient and horsepower may be predicted and optimized.

REFERENCES

BENTWICH, M., KELLY, D. A. I. & EPSTEIN, N. 1966 *J. Basic Eng.* (*ASME*). Submitted.
BERKOWITZ, N., BROWN, R. A. S. & JENSEN, E. J. 1965 *Can. J. Chem. Eng.* **43**, 280–5.
CALDWELL, J. 1930 *J. Roy. Tech. Coll. Glasgow*, **2**, 203–20.
CHARLES, M. E. 1963 *Can. J. Chem. Eng.* **41**, 46–51.
ELLIS, H. S. 1964*a* *Can. J. Chem. Eng.* **42**, 1–8.
ELLIS, H. S. 1964*b* *Can. J. Chem. Eng.* **42**, 69–76.
ELLIS, H. S. 1964*c* *Can. J. Chem. Eng.* **42**, 155–61.
ELLIS, H. S. & BOLT, L. H. 1964 *Can. J. Chem. Eng.* **42**, 201–6.
HODGSON, G. W. & CHARLES, M. E. 1963 *Can. J. Chem. Eng.* **41**, 43–5.
NEWTON, R., REDBERGER, P. J. & ROUND, G. F. 1964 *Can. J. Chem. Eng.* **42**, 168–73.
ROUND, G. F. & BOLT, L. H. 1965 *Can. J. Chem. Eng.* **43**, 197–205.